

## Introduction

Dorsal root ganglion (DRG) neurons transfer sensory signals from the peripheral to the central nervous system. Understanding the electrophysiological properties of DRG neurons has a significant application for pain research and potential drug development. Given the limited availability of human DRG neurons, the development of human-induced pluripotent stem cell (hiPSC)-derived sensory neurons (SNs) that contain DRG neuron electrophysiological properties provides a promising way to perform in vitro pain research. In addition, the latest expansion of automated patch clamp (APC) into a 384-well format provides the possibility of a high throughput screening (HTS) for thousands of compounds. In this study, RealDRG™ hiPSC-derived SNs were produced at massive scale and consistency to meet the demands of high-throughput APC studies. These SNs bear similarities to human DRG from a whole-transcriptome perspective and have been previously shown to possess functional voltage and ligand-gated channels important for nociception via manual patch clamp. To show the utility of nociceptors in HTS APC, we investigated the electrophysiological properties of hiPSC derived SNs on the Qube 384 APC system over time spans of 9-, 14-, 21-, and 28-day cultures. Using an optimized cell dissociation protocol to obtain healthy cell membranes for patch-clamp, we obtained a whole-cell success rate of 40.69-53.19%. Among these cells, 90.54-97.22% expressed K<sub>v</sub> currents, and 59.76-77.48% expressed Nav currents. For the Nav current group, 30.7-37.5% of cells carried a detectable TTX-resistant component. Furthermore, under current clamp mode, action potential firings were recorded from 60.12-66.76% of the cells that passed the success filter criteria.

## Materials and methods

### Cell culture

**Manufacture of RealDRG™.** RealDRG™ (Anatomic, 7009) were manufactured from hiPSCs using a novel, 7-day directed differentiation protocol, commercially available as Senso-DM (Anatomic, 70007) as previously described<sup>1</sup>.

**Culture of RealDRG™.** Tissue-culture treated plastic was pre-coated with Matrix 3 (Anatomic, M8003) for a minimum 2 hours prior to thaw. RealDRG™ were thawed and resuspended in Senso-MM (Anatomic, 7008) and seeded at a density of approximately 100K cells/cm<sup>2</sup>. Cultures were maintained for one, two, three, and four weeks during which two-thirds media exchanged every other day. For dissociation prior to running on APC, papain solution (Worthington, LK003178) was prepared according to manufacturer's instructions and diluted to 3 U/mL into Senso-MM. This solution was incubated with RealDRG™ overnight to gently dissociate neuronal axons. The resulting culture was collected and triturated vigorously using a P1000 pipet to create free-floating soma, diluted 1:4 in DMEM F-12, and centrifuged for 3 minutes at 300 x G. The resulting pellet was resuspended in extracellular solution for running on APC.

### Calcium Imaging

RealDRG™ cultures that had been matured for 4 weeks were loaded with 2.5 μM Calbryte 520 AM (AAT Bioquest, 20651) and PowerLoad Concentrate (1:100, ThermoFisher Scientific, P10020) for 1 h before imaging as described previously<sup>1</sup>. Time-based imaging was acquired using a Leica DMI6000B microscope, a DFC365FX camera, and a 10x air objective (NA 0.25, Leica Microsystems) for a duration of 185 s at four frames per second. Drug solutions were added to the cultures within the first 10 s of each video, which included 500nM capsaicin (TCI America™, M11491G), 10 μM capsazepine (Tocris, 0464), and 0.1% DMSO as negative control.

### Automated patch clamp for electrophysiology recording

**Solutions and blockers:** Extracellular solution (mM): NaCl 145, CaCl<sub>2</sub> 2, MgCl<sub>2</sub> 1, KCl 4, HEPES 10, and Glucose 10, pH = 7.4. Intracellular solution (IC) in mM: KF 120, KCl 20, HEPES 10, and EGTA 10, pH = 7.2. CsF internal solution (mM): CsF 135, NaCl 10, HEPES 10, EGTA 1.0, pH7. Tetrodotoxin (TTX) 0.5μM (Alomone Labs) and A-803467 (Millipore-Sigma) 1μM or 10μM were used for Na channel characterization.

**Voltage- and current-clamp protocols:** With holding voltage at -90mV, voltage step protocol consisted of a 200 ms pre-step at -120 mV and followed by 500 ms voltage steps from -90 mV to +80 mV with 10mV increment. For the blocker adding liquid period, a single pulse protocol was applied as: V<sub>h</sub>=-90mV, depolarized to -10mV, 20ms after 200ms pre-step at -120mV. In step current clamp, holding voltage at -90mV, followed by a sequential 10pA stepwise current injection. The ramp current clamp was elicited by injecting current from -100pA to 100pA with 500 or 1000ms duration.

**Analysis:** All the experiments were first filtered by seal success rate (membrane resistance R<sub>m</sub> > 200 MΩ) and then the size of cell (cell capacitance C<sub>cell</sub> > 2 pF). Current measurements were only performed on the wells fulfilled both criteria.

## Summary

These preliminary results present the fundamental electrophysiological recordings of hiPSC-derived SNs obtained from APC system, including action potentials and current-voltage characteristics of Na<sub>v</sub> and K<sub>v</sub> channels. Our data demonstrate the feasibility of performing high-throughput compound screening with the combining of well-developed hiPSC-derived sensory neurons and automated patch clamp.

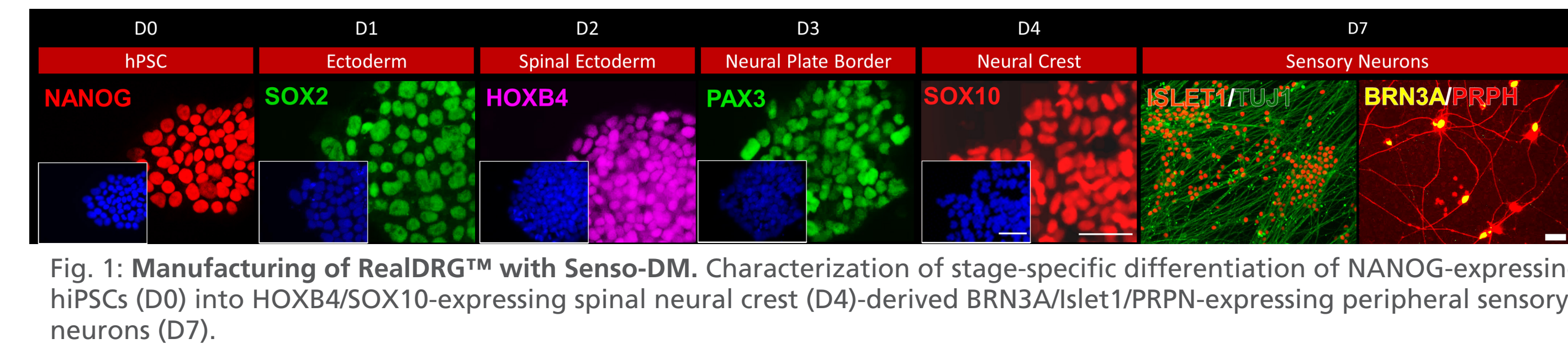


Fig. 1: Manufacturing of RealDRG™ with Senso-DM. Characterization of stage-specific differentiation of NANOG-expressing hiPSCs (D0) into HOXB4/SOX10-expressing spinal neural crest (D4)-derived BRN3A/Islet1/PRPN-expressing peripheral sensory neurons (D7).

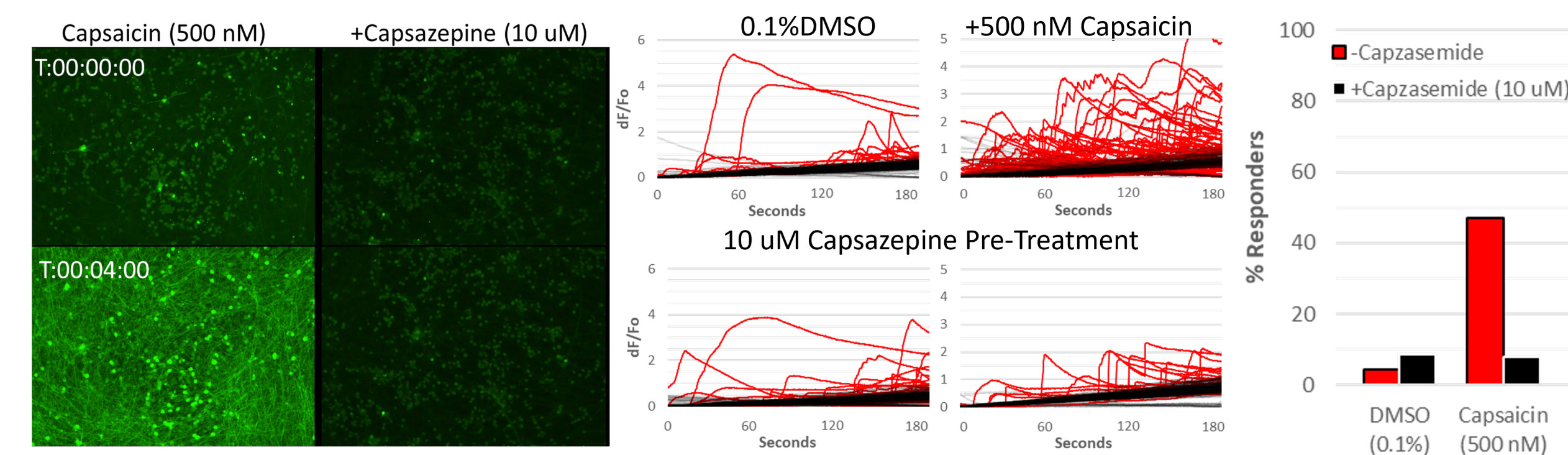


Fig. 2: Characterization of RealDRG™ Capsaicin Responses. Following 4 weeks in culture, approximately 45% of RealDRG™ soma respond to capsaicin by calcium imaging. Cultures fail to respond to capsaicin in the presence of the TRPV1 selective antagonist capsazepine, suggestive of a TRPV1-specific calcium response. The intensity profiles are graphed as ΔF/F<sub>0</sub>, ΔF is the intensity differential compared with background fluorescence (F<sub>0</sub>) of the given sample. Responders were mathematically defined by the maximum of the first derivative of its fluorescent intensity over time above a constant threshold that was determined by that of the background fluorescence over time.

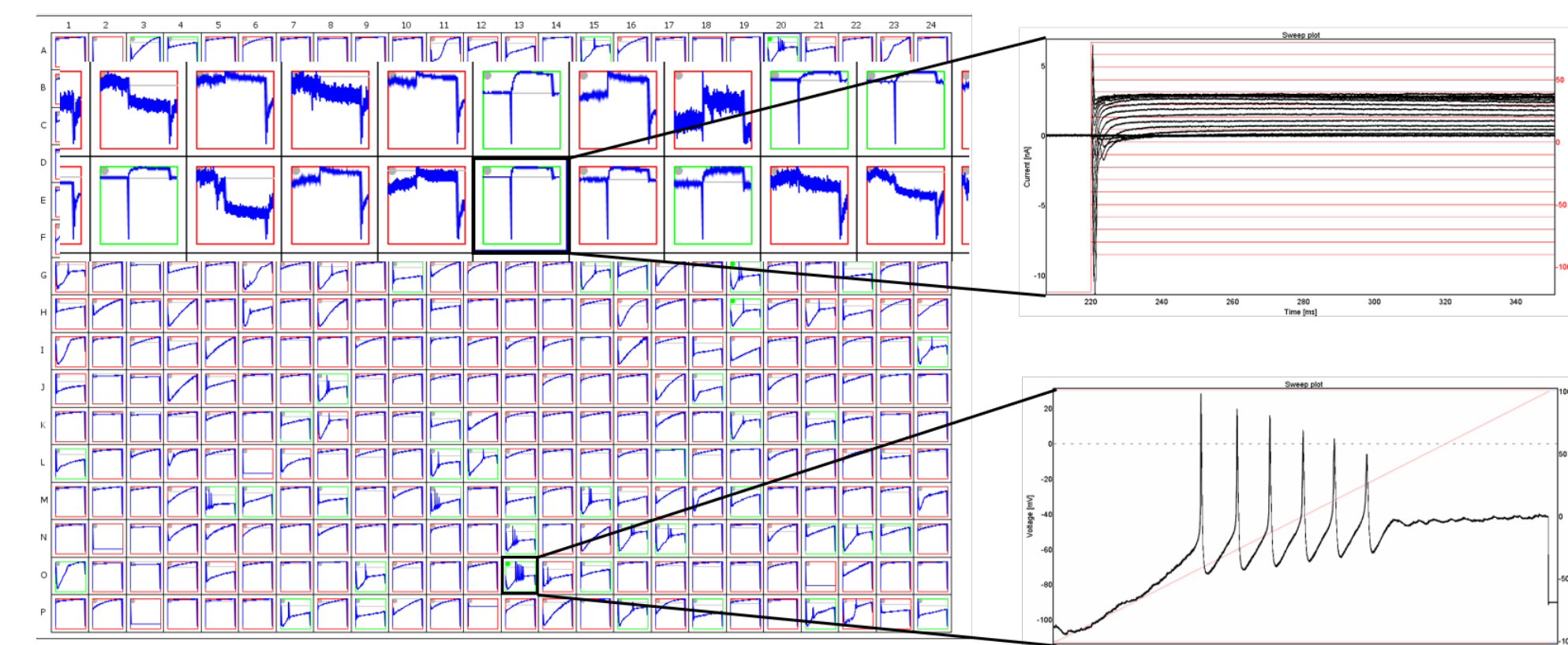


Fig. 3: Screening of hiPSC derived sensory neurons on Qube 384. Background is a Qchip view of 384 well setting with current-clamp ramp protocol: cells were holding at -90mV, followed with a -100pA to +100 pA current injection for 1s. The enlarged panel shows one cell with multiple action potential firings. The top overlay is a cut-out part of 384 wells for voltage clamp with the protocol of V<sub>h</sub>=-90mV, pre-step to -120mV for 200ms, followed by depolarization from -90 to +60mV for 500ms. Green and red borders correspond to the passed and failed experiments, respectively, with which the passing criteria were R<sub>mem</sub> > 200 MΩ and C<sub>cell</sub> > 2 pF.

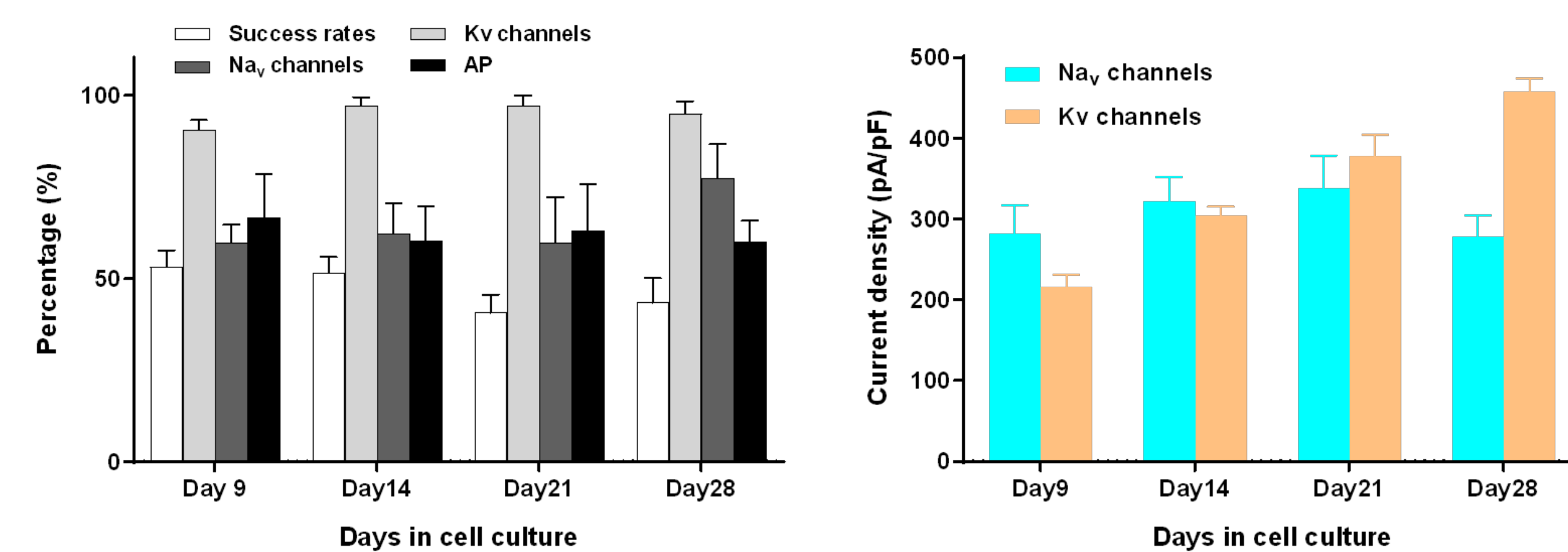


Fig. 4: Qube384 experiment success rates and current expression levels of hiPSC derived SNs during culture period of 28 days. Left: success rate indicates all the cells passed the criteria of R<sub>mem</sub> > 200 MΩ, the rates were decreased with longer culture period, which are 53.19±4.48% (n=3), 51.56±4.38% (n=3), 40.69±4.94% (n=4), and 43.45.19±6.65% (n=4), respectively, for time span of 9, 14, 21, and 28 days. For the cells passed membrane resistance and cell size filters, expression level of Kv channels is 90%-97% for all four culture time points, whereas only 60%-77% for Nav channels and 60%-67% for action potential firing were observed in the same group of cells. Right: Current densities were measured at depolarizations to -10mV, 20ms for Nav channels, and +60mV, 500ms for Kv currents. There is not difference among the four time-span groups for Nav current density, which are 281.99±35.35pA/pF (n=42), 322.75±29.66pA/pF (n=103), 338.52±40.08pA/pF (n=46), and 278.88±25.54 (n=125), respectively, for D9, D14, D21, and D28. However, Kv current densities increased with the increasing days of culture, which are 215.91±15.34pA/pF (n=55), 305.16±10.06pA/pF (n=138), 378.29±26.61pA/pF (n=68), and 457.47±16.30pA/pF (n=163).

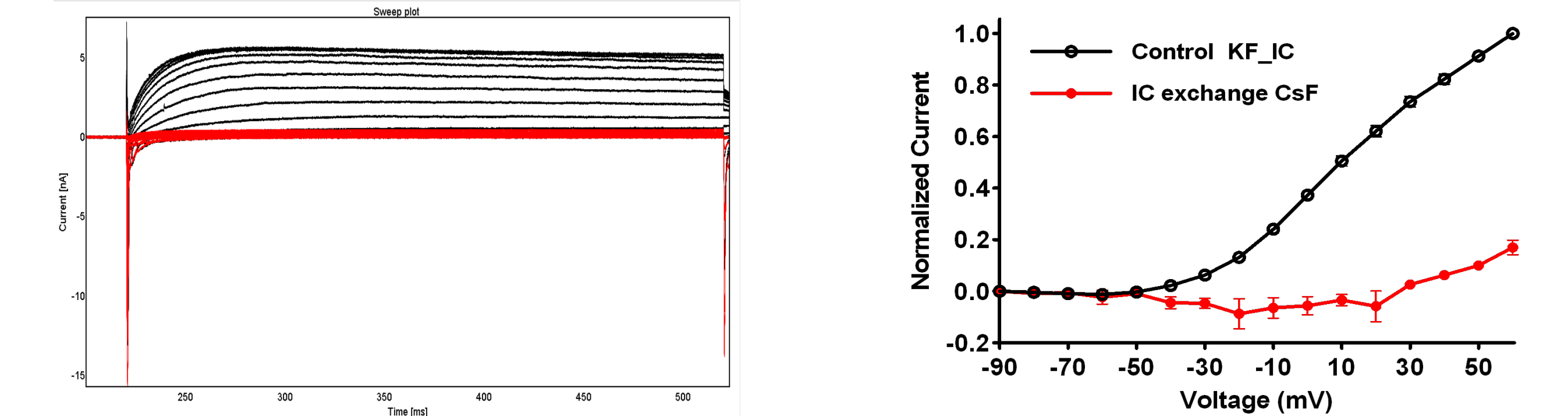


Fig. 5: Current-voltage relationship curves for Kv channels. Left: family current traces with internal solution of KF (black) and after exchanging to CsF based internal solution (red). Currents were elicited by 10mV stepwise voltage increasing from -90mV to +60mV for 300ms. Right: current-voltage curves were all normalized to the current amplitudes at +60mV before IC exchange.

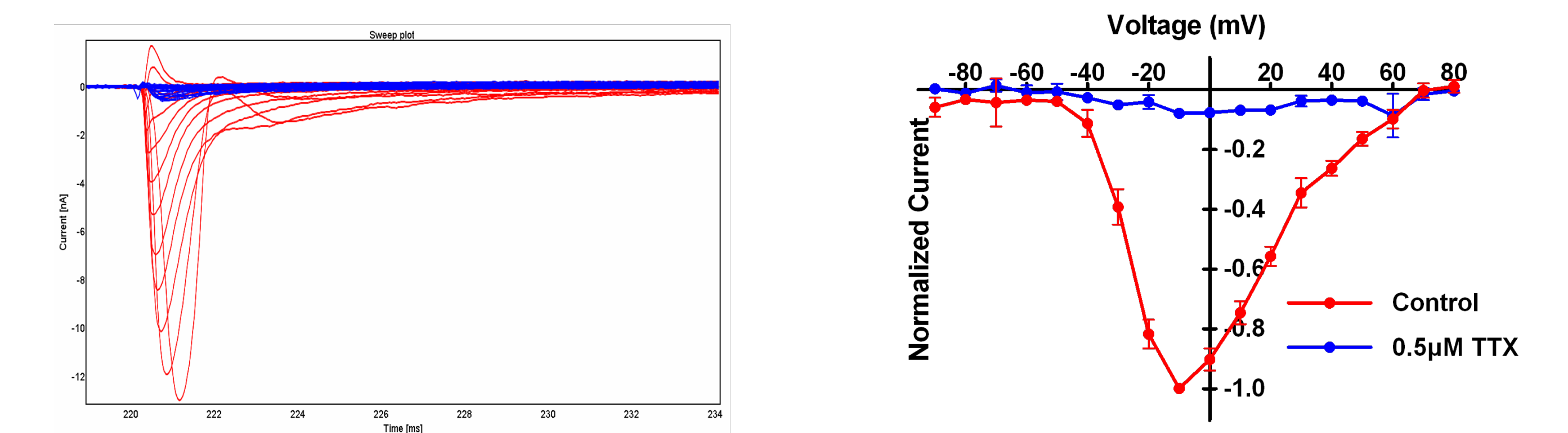


Fig. 6: Characterization of TTX sensitive Na<sub>v</sub> channels. Left: family of current traces in control and 0.5μM TTX groups by using the same voltage protocol described previously. Right: current-voltage relationship curves, all the current amplitudes were normalized to the control currents at the voltage of -10mV (Data showed was from day14 cells).

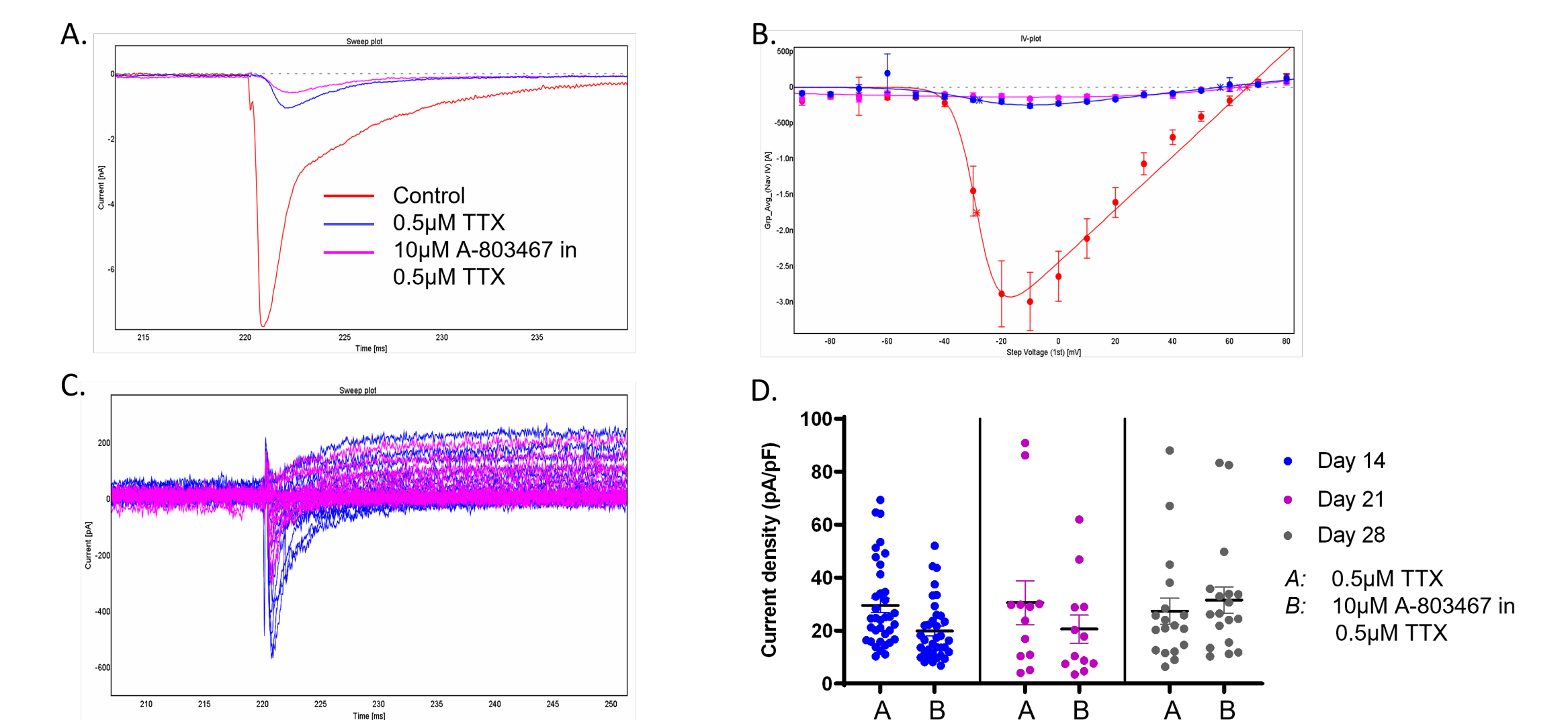


Fig. 7: Pharmacological evaluation of residual currents after 0.5μM TTX application. A: current traces at voltage -10mV for control, 0.5μM TTX, and 10μM A-803467 in 0.5μM TTX. B: Family of currents on the same cell before (blue) and after 10μM A-803467 (purple) in the presence of 0.5μM TTX. Same voltage protocol was applied as previous. C: Representative group average IV curves from day 21 cells for control (red), 0.5μM TTX (blue), and 10μM A-803467 in 0.5μM TTX (purple). D: Current densities significantly decreased by adding 10μM A-803467 after application of 0.5μM TTX, which are 29.55±2.67pA/pF vs 19.84±1.86pA/pF (n=36) and 30.56±7.95pA/pF vs 20.59±5.05pA/pF (n=12), respectively, for day 14 and day 21. However, a slightly increase of current densities was observed for day 28 cells, which are 27.34±4.82pA/pF vs 31.51±4.89pA/pF (n=18).

## References

Li R, Walsh P, Truong V, Petersen A, Dutton JR, Hubel A. Differentiation of Human iPS Cells Into Sensory Neurons Exhibits Developmental Stage-Specific Cryopreservation Challenges. *Front Cell Dev Biol.* 2021;9:796960. Published 2021 Dec 14. doi:10.3389/fcell.2021.796960